JOURNAL OF MOLECULAR SPECTROSCOPY 166, 354–364 (1994)

The Microwave Spectrum and Structure of the Argon–Acetaldehyde van der Waals Complex

IOANNIS I. IOANNOU* AND ROBERT L. KUCZKOWSKI†

Department of Physics and †Department of Chemistry, University of Michigan, Ann Arbor, Michigan 48109-1055

The argon–acetaldehyde van der Waals dimer was studied by Fourier transform microwave spectroscopy. Two tunneling motions were observed in the spectrum, an inversion through a planar configuration and methyl internal rotation. A simple deperturbation technique was employed in order to obtain rotational constants for structural purposes. The structure was found to be a nonplanar skew, with the argon binding on top of the C–C–O triangle. This was determined by assigning the rotational spectrum of two isotopic species: normal and Ar · CH_3CDO. The argon atom is located 3.592(5) Å from the acetaldehyde center of mass, and the distances Ar–$O_{carbonyl}$, Ar–$C_{carbonyl}$, and Ar–C_{methyl} are 3.59(1), 3.77(1), and 3.85(1) Å, respectively. The dipole moment was determined as μ = 2.63(2) D. An induction model was employed to explain the decrease in the dipole moment compared to free acetaldehyde. A dispersion model was used to rationalize the structural data. The binding energy of the dimer was estimated to be 204(1) cm^{-1} from centrifugal distortion data and a Lennard–Jones potential.

1. INTRODUCTION

Acetaldehyde is a small organic molecule with low symmetry. Although there are many known dimers of a rare gas with nonpolar or polar molecules, there are few examples with asymmetric organic species like acetaldehyde. Such systems are of interest because the rare gas provides a spherical test probe of the electron density and resultant electric fields which influence van der Waals interactions. It is desirable to learn if such interactions will track with chemical functionality and be transferable in a predictable fashion to more complex systems.

Two examples of pertinent argon complexes with organic molecules previously explored are Ar · formamide (*1*) and Ar · formic acid (*2*). The former is nonplanar while the latter is planar (or nearly so), with the argon straddling the acidic hydrogen and carbonyl oxygen. This indicates that the carbonyl group which is common to formamide and formic acid is not a helpful qualitative predictor of whether Ar · CH_3CHO will be planar or nonplanar. On the other hand, a simple physical model based on pairwise dispersion interactions (*3*) between the atomic centers of the molecule and the rare gas predicts a nonplanar structure for argon–acetaldehyde, with the argon roughly equidistant to the three heavy atoms (see below). This model has been fairly successful at rationalizing the structures of a number of rare gas complexes but has not been widely tested for less symmetric systems such as Ar · acetaldehyde, no doubt due to a paucity of experimental data.

We have observed the rotational spectrum of Ar · CH_3CHO in a Fourier transform microwave spectrometer with a pulsed nozzle source. The derived structure of Ar · CH_3CHO is close to the dispersion model prediction. The spectrum was quite complex, being perturbed by internal rotation of the methyl group and a tunneling motion through a planar configuration, giving quartets. Because of the complexity of

0022-2852/94 $6.00

the spectrum, this work will be reported in two parts. This paper describes a "deperturbed" spectral analysis to obtain unsplit frequencies which can be fit reasonably well by a standard Watson semirigid rotor Hamiltonian. This is sufficient to produce rotational constants and dipole moment components for understanding the structural parameters for the argon–acetaldehyde complex. The nonrigidity of the complex will be discussed in a second paper (*4*). That analysis will extend the IAM formalism of Hougen–Coudert to the G_6 molecular symmetry group and describe a Hamiltonian which includes effects from methyl internal rotation and an inversion motion.

2. EXPERIMENTAL DETAILS

Sample

The vapor of acetaldehyde (99%, Aldrich) was mixed with argon in a 2-liter bulb at a total pressure of 1–1.5 atm. The ratio of acetaldehyde to argon was about 1.5:98.5. The sample was then expanded supersonically through a modified Bosch fuel injection valve with a 1-mm orifice to form the dimer. Transitions of argon–acetaldehyde-d_1 (CH_3CDO) were observed using deuterium-enriched acetaldehyde (98+% D, Aldrich).

Spectrometer

The spectrum in the range 7.3–18 GHz was investigated using a Balle–Flygare pulsed FTMW spectrometer described previously (*5*). The rest of the spectrum, in the range 3–7.3 GHz, was obtained with a second recently constructed Balle–Flygare pulsed FTMW spectrometer. Stark effects were obtained by applying electric potentials up to 8000 V with opposite polarity to two wire mesh parallel plate screens separated by about 30 cm which straddled the Fabry–Perot cavity. Maximum Stark shifts ranged from 2.3 MHz for the $A_1 \rightarrow A_2$ component of the 0_{00}–1_{10} quartet to 7.8 MHz for the $A_1 \rightarrow A_2$ component of the 1_{01}–2_{11} transition. The electric fields were calibrated using OCS (μ = 0.71519 D) (*6*).

Timing of the gas and MW pulses was adjusted so that the Doppler effect would be minimal on the lineshapes. The axis of the expansion was ordinarily perpendicular to the cavity axis, with the exception of some partially split lines (splitting smaller than the linewidth of the perpendicular configuration), in which case an axial nozzle was used to resolve the lines as much as possible. The linewidth for the perpendicular configuration was about 25 kHz except for cases where deuterium quadrupole coupling would broaden the line (to about 50 kHz). The axial configuration gave FWHM of about 10 kHz, with the line splitting into two components due to the Doppler effect. The line centers were estimated to be accurate to ±4 kHz.

3. RESULTS AND DISCUSSION

Spectrum

The spectrum consisted of quartets arising from all three selection rules (μ_a, μ_b, μ_c). The existence of three selection rules implies that the complex does not have a plane of symmetry, as does the argon–formic acid complex. Hence the argon must lie out of the plane defined by the heavy atoms in acetaldehyde.

A portion of the spectrum is illustrated in Fig. 1, which shows the typical quartet pattern for the three selection rules. As will be shown in a subsequent paper (*4*), each

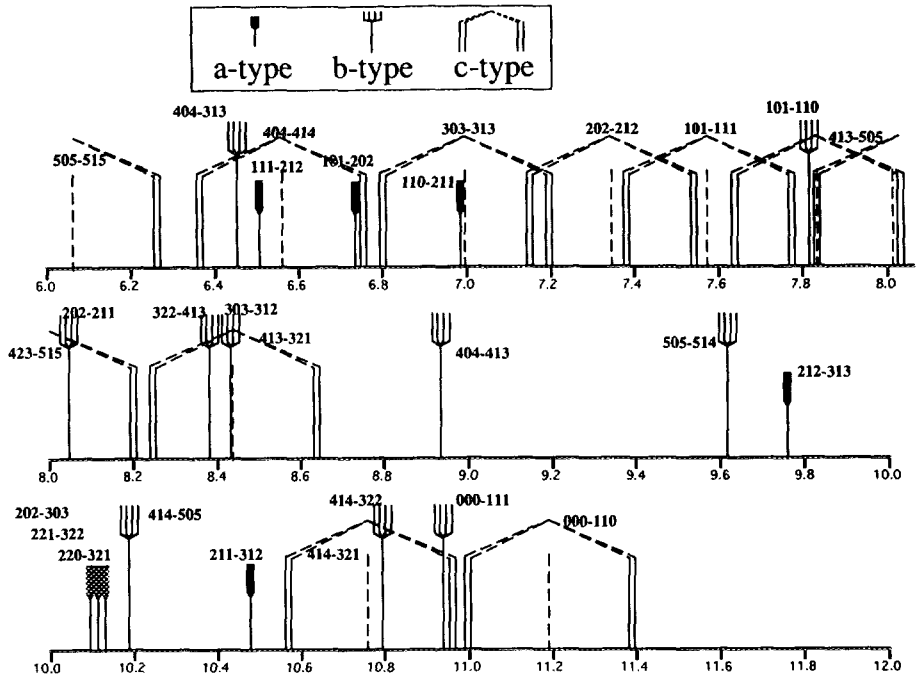

FIG. 1. Spectrum of Ar · CH_3CHO between 6 and 12 GHz.

quartet arises from the rigid rotor level first split by about 310 MHz into an A and E state due to tunneling of the methyl group through a threefold barrier. These are further split by about 90 MHz into two A states (actually A_1 and A_2) and two E states when the argon (effectively) tunnels from above the heavy atom plane to an equivalent position below the plane. Due to the symmetry of the levels and selection rules, this resulted in different patterns for the a-, b-, and c-type transitions. For b-type lines, the A–E splitting was typically 200 kHz, and the two A–E doublets were separated from each other by 2–10 MHz, depending on J. The a-type quartets were more closely spaced (typically within 1 MHz). The c-type lines, on the other hand, were split into two A–E doublets shifted by about 200 MHz above and below the respective asymmetric rotor frequency to which they correlate (the latter is shown by a dotted line in the figure). For the c-type lines the magnitude of the A–E splitting of each doublet was about 15 MHz and was shown to be sensitive to the coupling between the inversion and the methyl rotation.

One way to extract information about the moments of inertia is to average the four lines seen in place of the single asymmetric rotor frequency giving a weight of two to the E states. They can be shown (*4*) to be displaced by half the amount of the A states relative to the respective asymmetric rotor level. The resulting frequencies are tabulated in Table I along with the obs − calc frequency differences obtained from fitting the average frequencies to a Watson S-reduction Hamiltonian (I^r representation) (*7*). The parameters obtained from the fit are given in Table II. The fit to the average frequencies is not as good as a typical fit for a more rigid van der Waals system, but at worst it is off by only 0.5 MHz. This is sufficient to confirm the asymmetric rotor assignment and deduce structural information.

TABLE I

Rotational Transitions (in MHz) of the Tunneling Quartets of Ar · CH_3CHO and the Average Frequency[a]

$J'_{K'a}K'_c$-$J''_{K''a}K''_c$	A_1	E	A_2	E	Average[a]	o-c(kHz)[b]
1_{01}-0_{00}	3375.162	3375.056	3374.949	3374.849	3374.987	-24
2_{02}-1_{01}	6744.063	6743.874	6744.468	6744.268	6744.136	-39
2_{12}-1_{11}	6512.435	6512.026	6511.420	6511.420	6511.791	40
2_{11}-1_{10}	6986.136	6986.216	6986.216	6985.915	6986.102	-42
3_{03}-2_{02}	10102.092	10101.824	10101.537	10101.276	10101.638	-31
3_{13}-2_{12}	9762.942	9762.942	9763.061	9763.045	9762.996	46
3_{12}-2_{11}	10474.945	10474.493	10476.235	10475.754	10475.279	-38
3_{22}-2_{21}	10119.276	10119.157	10119.851	10119.851	10119.524	53
3_{21}-2_{20}	10141.636	10141.120	10140.967	10140.573	10140.998	-152
4_{04}-3_{03}	13441.671	13441.361	13442.324	13442.003	13441.787	1
4_{14}-3_{13}	13009.776	13009.776	13009.628	13009.648	13009.709	51
4_{13}-3_{12}	13959.959	13959.311	13958.224	13957.620	13958.674	20
4_{23}-3_{22}	13487.366	13487.061	13486.888	13486.617	13486.935	9
4_{22}-3_{21}	13540.830	13540.428	13541.505	13541.027	13540.874	-94
5_{05}-4_{04}	16759.750	16759.416	16759.082	16758.754	16759.195	65
5_{15}-4_{14}	16250.042	16250.087	16250.256	16250.277	16250.171	96
5_{14}-4_{13}	17434.078	17433.326	17436.222	17435.413	17434.630	85
1_{10}-1_{01}	7808.439	7808.258	7810.901	7810.216	7809.381	391
1_{11}-0_{00}	10946.906	10946.716	10944.704	10945.005	10945.842	-543
2_{11}-2_{02}	8052.577	8052.163	8050.589	8050.302	8051.349	13
2_{12}-1_{01}	14082.182	14082.182	14083.177	14083.083	14082.648	-116
3_{12}-3_{03}	8423.996	8423.520	8426.722	8426.099	8424.993	10
3_{13}-2_{02}	17101.651	17101.759	17101.193	17101.355	17101.512	-27
3_{13}-2_{20}	13670.129	13669.600	13667.541	13667.012	13668.482	-258
3_{12}-2_{21}	12237.775	12237.825	12237.523	12237.409	12237.628	57
4_{13}-4_{04}	8944.359	8943.408	8940.546	8939.776	8941.879	28
4_{04}-3_{13}	6442.020	6441.281	6442.760	6442.061	6441.911	-5
4_{14}-3_{21}	10798.732	10797.807	10802.140	10801.076	10799.773	-56
4_{13}-3_{22}	8397.428	8397.940	8398.825	8399.363	8398.476	27
5_{14}-5_{05}	9615.540	9614.345	9620.836	9619.407	9617.313	48
5_{05}-4_{14}	10192.884	10191.829	10191.324	10190.262	10191.398	9
5_{15}-4_{22}	8093.602	8092.015	8089.308	8087.963	8090.478	131
5_{14}-4_{23}	4451.642	4452.657	4448.569	4449.588	4450.784	99
6_{15}-6_{06}	10474.106	10472.019	10466.866	10465.081	10469.195	34
6_{06}-5_{15}	13990.102	13988.715	13992.466	13991.059	13990.353	77
7_{16}-7_{07}	11513.671	11511.112	11523.385	11520.431	11516.690	-66
1_{11}-1_{01}	7374.010	7388.906	7767.501	7752.911	7570.858	-516
1_{10}-0_{00}	11381.341	11366.070	10988.111	11002.311	11184.369	367
2_{12}-2_{02}	7535.469	7520.670	7141.375	7156.454	7338.515	-74
2_{11}-1_{01}	14599.300	14613.677	14992.393	14976.930	14795.484	-27
3_{13}-3_{03}	6802.778	6818.124	7196.441	7181.897	6999.877	7
3_{13}-2_{21}	13858.994	13843.225	13467.802	13481.612	13662.745	53
3_{12}-2_{20}	12048.908	12064.205	12437.259	12422.810	12243.366	-255
4_{14}-4_{04}	6763.896	6749.674	6370.734	6386.408	6567.799	58
4_{04}-3_{12}	5211.738	5197.081	4821.543	4836.664	5016.795	-8
4_{14}-3_{22}	10577.894	10591.677	10968.640	10952.736	10772.560	52
4_{13}-3_{21}	8618.268	8604.072	8232.326	8247.706	8425.692	-84
5_{15}-5_{05}	5861.690	5877.738	6254.402	6240.533	6058.772	85
5_{05}-4_{13}	7623.067	7638.457	8010.858	7996.527	7817.316	36
5_{15}-4_{23}	8205.489	8189.263	7815.006	7828.460	8009.323	139
5_{14}-4_{22}	4339.753	4355.409	4722.872	4709.089	4531.937	94
6_{16}-6_{06}	5687.976	5674.469	5295.557	5311.995	5492.744	105
6_{06}-5_{14}	10623.669	10609.841	10238.619	10254.453	10431.813	116
7_{17}-7_{07}	4694.729	4711.557	5087.143	5073.972	4892.155	134
7_{07}-6_{15}	12646.619	12663.105	13028.716	13013.802	12838.192	-331

[a] $\nu_{average} = (\nu_{A_1\text{-}A_2} + 2\nu_E + \nu_{A_2\text{-}A_1} + 2\nu_E)/6$. See text.

[b] $\nu_{obs} - \nu_{calc}$ where $\nu_{obs} = \nu_{average}$ and ν_{calc} was obtained from the constants in table II.

The spectrum of Ar · CH_3CDO was studied as well since the isotope shift can give additional information on the structure. These transitions were similarly split into quartets whose components were sometimes further split into doublets or triplets from deuterium quadrupole coupling (*8*). No attempt to determine the quadrupole coupling constants of the deuterium was made. However, the published coupling constants for the deuterated monomer species were used (*9*) to predict the spectral patterns. For

TABLE II

Fitted Parameters of the Average Frequencies for the Normal and Deuterated Isotopic Species

Parameter	Ar·CH_3CHO	Ar·CH_3CDO[a]
A (MHz)	9377.998(62)[b]	9035.927(12)
B (MHz)	1806.351(13)	1767.6809(42)
C (MHz)	1568.718(12)	1549.7779(42)
D_J (kHz)	14.34(20)	
D_{JK} (kHz)	181.0(18)	
D_K (kHz)	-80(11)	
d_1 (kHz)	-2.121(89)	
d_2 (kHz)	-1.62(22)	
κ	-0.93914	-0.94179
$\Delta\nu_{rms}$[c] (kHz)	188	31
No. of lines	55	12

[a]Distortion constants were held at the normal species values.
[b]The uncertainties in parentheses are 1σ.
[c]$\Delta\nu = \nu_{obs} - \nu_{calc}$.

the lines affected appreciably by quadrupole coupling, the strongest component was predicted to appear within 10 kHz of the unperturbed frequency and thus it was used in the averaging over the symmetry states (again the weight of the *E* states was two). The average frequencies for the four components were computed in a similar fashion to the normal species and are listed in Table III, along with the frequency fit ($\nu_{obs} - \nu_{calc}$) obtained with an *S*-reduced Watson Hamiltonian. The distortion constants were held at the normal species values. The rotational constants determined are given in Table II.

Structure

It can be shown in general that four structures result from fitting the rotational constants for one isotopic species of a rare gas complex (*1*). These four structures are

TABLE III

Rotational Transitions (MHz) for Ar–CH_3CDO and the Average Frequency of the Tunneling Quartets[a]

$J'_{K'_PK'_O}$-$J''_{K''_PK''_O}$	A_1	E	A_2	E	Average	o-c(kHz)[b]
1_{10}-1_{01}	7485.581	7485.505	7486.311	7486.183	7485.878	20
1_{11}-0_{00}	10585.605	10585.705	10585.025	10585.092	10585.371	-3
1_{11}-1_{01}	7199.514	7202.130	7336.431	7333.766	7267.956	-16
1_{10}-0_{00}	10871.794	10868.959	10734.993	10737.436	10803.263	3
2_{02}-1_{01}	6629.623	6629.467	6629.847	6629.688	6629.630	-4
2_{11}-1_{10}	6851.468	6851.206	6851.917	6851.668	6851.522	-48
2_{11}-2_{02}	7708.387	7708.164	7707.439	7707.246	7707.774	-20
2_{12}-2_{02}	7122.537	7120.022	6985.816	6988.584	7054.261	23
2_{11}-1_{01}	14269.526	14271.795	14405.766	14402.770	14337.404	-24
3_{03}-2_{02}	9931.908	9931.681	9931.599	9931.374	9931.603	51
3_{12}-3_{03}	8049.118	8048.779	8050.448	8050.072	8049.545	-18
4_{13}-4_{04}	8522.961	8522.384	8521.086	8520.522	8521.643	35

[a] See footnote a, table I.
[b] See footnote b, table I.

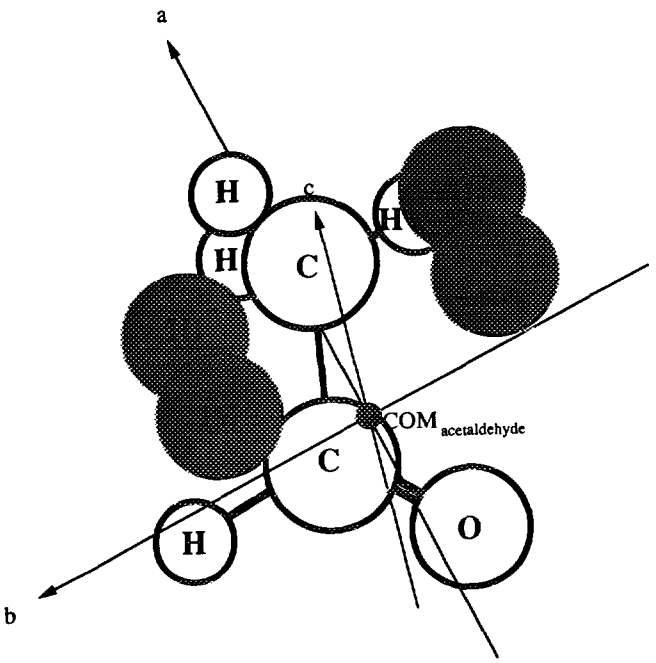

FIG. 2. Four equivalent inertial positions for argon, in the principal axis system of acetaldehyde, obtained from fitting moments of inertia of one isotopic species (normal isotope).

illustrated in Fig. 2, in the principal axis system of acetaldehyde monomer. The argon binds quite close to the *bc* plane of acetaldehyde (at a distance of about 0.25 Å); the picture exaggerates the distance from that plane. Inspection of the figure suggests that substitution of the aldehydic hydrogen with deuterium will have a marked effect on the spectrum and this is indeed true. The isotope shift for Ar · CH_3CDO is inconsistent with the aldehydic hydrogen lying close to the argon, eliminating structures III and IV.

TABLE IV

Selected Principal Axis Coordinates and Structural Parameters for Argon–Acetaldehyde

Coordinates(Å)	$\lvert a_o \rvert$ [a]	$\lvert a_s \rvert$ [b]	$\lvert b_o \rvert$	$\lvert b_s \rvert$	$\lvert c_o \rvert$	$\lvert c_s \rvert$
Hydrogen (H_{ald})	2.310	2.000	0.279	<0	1.389	1.467

Structural Parameters	R_{cm}=3.592(5) Å[c]			
Distances (Å)	$O_{carbonyl}$-Ar	$C_{carbonyl}$-Ar	C_{met}-Ar	H_{ald}-Ar
	3.59(1)	3.77(1)	3.85(1)	4.42(1)
vdW sum (Å)	3.38	3.70	3.70	3.20

[a] r_o coordinates from least squares fitting of 6 I's; ΔI_{rms} = 0.92 amu Å^2 where $\Delta I = I_x(calc) - I_x(exp)$.

[b] Kraitchman substitution coordinates (r_s) (10).

[c] Distance between the centers-of-mass of Ar and CH_3CHO. The perpendicular distance from Ar to the heavy atom plane is 3.28 Å.

TABLE V

Principal Axis Coordinates for Argon–Acetaldehyde, Structure I, from Least-Squares Fitting of the Six Moments of Inertia

	a[a]	b	c
$O_{carbonyl}$	-1.495	-1.155	0.233
$C_{carbonyl}$	-1.866	-0.179	-0.372
C_{methyl}	-1.775	1.235	0.156
$H_{aldehyde}$	-2.310	-0.279	-1.389
$H_{1,methyl}$	-1.327	1.220	1.154
$H_{2,methyl}$	-2.778	1.666	0.211
$H_{3,methyl}$	-1.154	1.833	-0.515
Ar	1.882	0.032	-0.015

[a] Units are Å.

Shown in Table IV are the Kraitchman substitution coordinates (*10*) for the aldehydic hydrogen as well as the coordinates obtained from least-square fitting of the six moments of inertia holding the structure of acetaldehyde fixed to the published one (*11*). Structure I yielded the best standard deviation (σ = 0.92 amu · Å^2), with structure II the next best at 0.98 amu · Å^2, while the other two fit much worse (σ = 1.68 and 1.73 amu · Å^2 for III and IV, respectively). It is not possible to choose between structures I and II with the inertial data alone. However, the dipole analysis in the next section convincingly argues that structure I is the only viable choice. The Cartesian coordinates for the atoms for structure I are given in Table V.

Structure I is illustrated in Fig. 3 and various distances and angles are summarized in Table IV. The distance of the argon from the heavy atoms compared to the sum of the van der Waals radii shows no surprises. It can be seen that the argon sits above the O–C–C triangle, pulled somewhat toward the carbonyl bond. The perpendicular

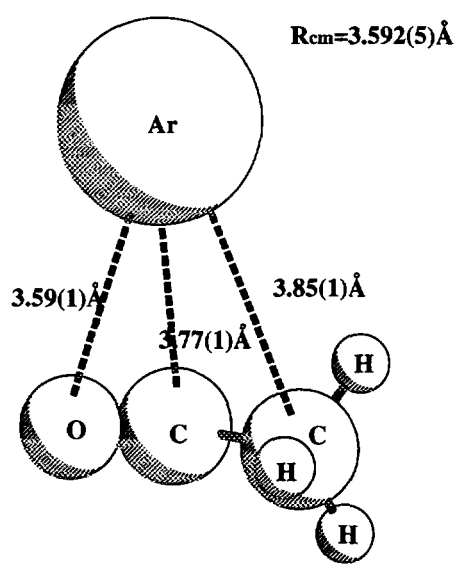

FIG. 3. Structure of Ar · CH_3CHO.

TABLE VI

Stark Coefficients ($\Delta\nu/E^2$)[a] of Argon–Acetaldehyde

		|M|	obs[a]	obs-calc[b]
2_{11}-1_{01}	$A_1 \rightarrow A_2$	1	0.796	0.017
2_{12}-2_{02}	$A_1 \rightarrow A_2$	2	0.406	0.013
2_{12}-2_{02}	$A_1 \rightarrow A_2$	1	0.979	-0.018
1_{11}-0_{00}	$A_1 \rightarrow A_2$	0	2.1252	0.0000
1_{10}-0_{00}	$A_1 \rightarrow A_2$	0	0.6429	-0.0009

[a] Second order Stark coefficient in 10^{-4} MHz/(V/cm)^2.
[b] Observed-calculated Stark coefficients. The latter were calculated using rotational constants in table II and the dipole components listed in table VII.

TABLE VII

Dipole Moment Components for Argon–Acetaldehyde

	Experimental[a]	Structure I[b]	Structure II
μ_a	0.532(42)	0.694	0.204
μ_b	2.401(13)	-2.453	-2.548
μ_c	0.930(32)	0.989	0.970
μ_{total}	2.629(18)	2.7341	

[a] Errors represent 1σ. All values in Debyes.
[b] Projection of the acetaldehyde monomer dipole moment in the principal axis system of the dimer.

distance of argon to the heavy atom plane is 3.28 Å. The angle between the R_{cm} vector and the acetaldehyde heavy atom plane is 66°. The orientation of the methyl group is not known, but presumably it is not distorted from free acetaldehyde where a C–H bond eclipses the carbonyl.

The least-squares structural fit is not very impressive. The large uncertainty must arise from large-amplitude vibrational effects coming from the tunneling motions and other vibrations. The more complete spectral analysis of the tunneling splittings (*4*), while improving the spectral fits and partially compensating for Coriolis effects, did not lead to an improved structural fit, so structure I is considered the best structure at this time. The uncertainties in Fig. 3 and Table IV are the statistical values from the least-squares fit and the structural parameters are the so-called r_0 parameters averaged over the vibrational motions which affect the rotational constants. It is not easy to estimate how close these parameters are to the equilibrium structure r_e without knowledge of the vibrational potential function. We propose that the uncertainties relative to the equilibrium values are about ±0.05 Å for the various distances.

Dipole Moment

Measurement of the Stark splittings was complicated by the tunneling splittings and perturbations which led to nonlinear $\Delta\nu$ vs E^2 behavior. The five A-state transitions

listed in Table VI were identified to have Stark shifts linear with E^2. These resulted in the dipole components given in Table VII. The dipole components vary slightly with the A state chosen for measurement, but this variation is covered by the estimated uncertainties.

In Table VII, the dipole components of Ar · CH_3CHO are compared with those expected for structures I and II by projecting the dipole moment of acetaldehyde (*12*) on the principal axis of the dimer. Since changes in the dipole components in rare gas complexes due to vibrational averaging and polarization effects are typically small (~0.1–0.2 D), it is apparent that structure I is preferred.

Dispersion Model

A simple dispersion model has been proposed to rationalize the structures of rare gas dimers (*3*). Its qualitative and even quantitative predictions were quite successful for most of the examples, with the exception of linear dimers, which usually involve molecules with acidic hydrogens. It employs a potential function which consists of a dispersive attractive part and a hard spheres repulsive part. The first term is of the form

$$E_{\text{attr}} = -\frac{3}{2}\alpha_{\text{rg}} \sum_{i}^{n_a} (r^a_{\text{cov},i})^3 R^{-6}_{\text{rg},i},$$

where the covalent radii (r_{cov}) are used as a measure of the atomic polarizability in the r^6 attractive term and α_{rg} is the rare gas polarizability. The sum extends over all atoms of the monomer. The repulsive term is represented by

$$E_{\text{rep}} = \frac{A}{2} \sum_{i}^{n_a} \left\{ 1 + \tanh\left[\frac{s_{\text{rg},i} - R_{\text{rg},i} - c}{d} \right] \right\},$$

where A, c, and d are shape factors defined in the original paper to analytically approximate the hard-sphere repulsion, and $s_{\text{rg},i}$ is the sum of the vdW radii of the rare gas and any one of the atoms of the monomer. The computer program based on the model is parametrized to search for a minimum energy structure according to the above prescription.

This model gave a minimum energy structure close to the observed structure. The parameters involved in the calculation are listed in Table VIII along with a comparison of the Ar distances to the carbon and oxygen atoms shown in Table IX. This reasonable agreement with structure I was very helpful in the early stages of this study for spectral prediction purposes. In fact, the spectrum predicted from this simple model led to the assignment of the $0 \rightarrow 1$, b- and c-type lines. Since a planar model was initially preferred, this helped to point the assignment in the proper spectral direction. One can see from Table VIII that the largest attractive contribution comes from the carbonyl. Also, the repulsive center at the center of the carbonyl bond provides most of the repulsive contribution which justifies its otherwise arbitrary use. Finally, we note the significant attractive contribution of the methyl hydrogen closest to the argon. The latter is interesting since it can be shown (*4*) that there is spectral evidence for a coupling between the two internal motions present in the system.

Binding Energy

Using a pseudodiatomic model, the stretching force constant and stretching frequency can be estimated from the equations

TABLE VIII

Dispersion Modeling of Argon–Acetaldehyde[a]

Atom	x(Å)	y(Å)	z(Å)	r^3_{cov}(au)	r_{vdW}(Å)	E_{attr}(au)	E_{rep}(au)
$O_{carbonyl}$	-1.142	-0.235	0.000	2.700	1.38	-0.00047	0.00000
Rep. center	-0.636	0.094	0.000	0.000	1.61	0.00000	0.00004
$C_{carbonyl}$	-0.130	0.423	0.000	3.100	1.56	-0.00035	0.00000
C_{methyl}	1.264	-0.163	0.000	3.100	1.70	-0.00039	0.00002
H_{ald}	-0.179	1.536	0.000	0.505	1.20	-0.00002	0.00000
H_{methyl}	1.199	-1.254	0.000	0.505	1.20	-0.00014	0.00000
H_{methyl}	1.798	0.173	-0.893	0.505	1.20	-0.00001	0.00000
H_{methyl}	1.798	0.173	0.893	0.505	1.20	-0.00008	0.00000
Ar	-0.171	-2.130	2.879	11.080	2.00		
					totals:	-0.00146	0.00006
					E_{int}:	-0.00140	

[a] See text and ref 3.

$$D_J = \frac{\hbar^4}{2h}\frac{\mu}{f_s(I^e)^3} = \frac{4B_e^3}{\omega_s^2}$$

as 0.023(1) mdyn/Å and 43(1) cm^{-1}, respectively, using the spectral constants for B and D_J in Table II. The binding energy was calculated from the equation

$$\epsilon = f_s r_e^2/72 \approx f_s R_{cm}^2/72$$

as ϵ = 204(1) cm^{-1}, assuming a 6–12 Lennard–Jones potential. Since the distortion and rotational constants are probably affected by the large-amplitude tunneling motions, one should be cautious in comparing the binding energy with other van der Waals dimers calculated similarly. Nevertheless, this appears to be a rather strong complex. For comparison, the binding energies for Ar · HCl (126.3 cm^{-1}) (*13*), Ar · formamide (126.5 cm^{-1}) (*1*), and Ar · formic acid (144.4 cm^{-1}) (*2*) are somewhat smaller.

TABLE IX

Experimental and Model Distances of Argon from Selected Acetaldehyde Atoms from the Dispersion Model[a]

Distance	Model [a]	Experimental
Ar - $O_{carbonyl}$	3.581 Å	3.589 Å
Ar - $C_{carbonyl}$	3.848	3.771
Ar - C_{methyl}	3.771	3.853

[a] See text and ref 3.

4. SUMMARY

The $Ar \cdot CH_3CHO$ complex has a nonplanar structure, with the Ar roughly over the C–C–O triangle. This structure appears to result from a balance between attractive dispersion forces and steric repulsions from the acetaldehyde atoms, according to the simple model of Kisiel (*3*). This model agreement suggests that his algorithm can be a valuable guide for predicting structures and rotational spectra for rare gas complexes with relatively complicated nonsymmetric organic systems. Nevertheless, more tests are desirable since Ar · HCOOH was a less successful system until some adjustments were made (adjustments in the radii used for the atomic centers and the repulsive center) (*2*).

It is of note that the analysis of the spectrum could proceed in a straightforward fashion despite two tunneling motions leading to splittings. This arose because a simple "deperturbation" technique could be employed, giving average unperturbed frequencies. This is suggestive of high barrier tunneling processes which split the spectrum but do not lead to large asymmetric shifts. The tunneling processes and barrier information will be addressed in a subsequent paper (*4*).

5. ACKNOWLEDGMENTS

We acknowledge the National Science Foundation, Experimental Physical Chemistry Program, for funding of this research. We are grateful to Professor Z. Kisiel for providing us with a program for performing the dispersion calculations and for some helpful discussions, and to Dr. Kurt W. Hillig III for advice during various stages of this project. The assistance of Dr. Jon T. Hougen in aspects of this study is also acknowledged.

RECEIVED: April 5, 1994

REFERENCES

1. R. D. SUENRAM, G. T. FRASER, F. J. LOVAS, C. W. GILLIES, AND J. ZOZOM, *J. Chem. Phys.* **89,** 6141–6146 (1988).
2. I. I. IOANNOU AND R. L. KUCZKOWSKI, *J. Phys. Chem.* **98,** 2231–2235 (1994).
3. Z. KISIEL, *J. Phys. Chem.* **95,** 7605–7612 (1991).
4. I. I. IOANNOU, R. L. KUCZKOWSKI, AND J. T. HOUGEN, in preparation.
5. K. W. HILLIG II, J. MATOS, A. SCIOLY, AND R. L. KUCZKOWSKI, *Chem. Phys. Lett.* **133,** 359–362 (1987).
6. K. TANAKA, H. ITO, K. HARADA, AND T. TANAKA, *J. Chem. Phys.* **80,** 5893–5905 (1984).
7. J. K. G. WATSON, *J. Chem. Phys.* **46,** 1935–1949 (1967).
8. I. I. IOANNOU, Ph.D. Thesis, University of Michigan, 1993.
9. L. MARTINACHE AND A. BAUDER, *Chem. Phys. Lett.* **164,** 657–663 (1989).
10. J. KRAITCHMAN, *Am. J. Phys.* **21,** 17–24 (1953).
11. T. IIJIMA AND S. TSUCHIYA, *J. Mol. Spectrosc.* **44,** 88–107 (1972).
12. W. BOSSERT, J. EKKERS, A. BAUDER, AND HS. H. GUNTHARD, *Chem. Phys.* **27,** 433–463 (1978).
13. S. E. NOVICK, K. C. JANDA, S. L. HOLMGREN, M. WALDMAN, AND W. KLEMPERER, *J. Chem. Phys.* **65,** 1114–1116 (1976).